J. Fluid Mech. (1983), *vol.* 129, *pp.* 173–192
Printed in Great Britain

Heat transfer and horizontally averaged temperature of convection with large viscosity variations

By FRANK M. RICHTER,†
Department of Earth Sciences, Cambridge University, England

HENRI-CLAUDE NATAF
California Institute of Technology, Pasadena

AND STEPHEN F. DALY
Jet Propulsion Laboratory, Pasadena, California

(Received 14 May 1982)

Experiments with fluids whose viscosity depends strongly on temperature are used to study the effect of viscosity variations in the range 10–10^5 on the heat transfer and horizontally averaged temperature of a convecting layer between horizontal isothermal boundaries. At large viscosity variations (3×10^3 and 10^5) and Rayleigh numbers less than the critical value given by linear theory, the system can be either conductive or convective depending on whether the Rayleigh number is increased from an earlier conductive state or decreased from a preexisting convective state. At higher Rayleigh numbers and for the entire range of viscosity variation studied the heat transfer differs little ($< 20\%$) from that of a uniform-viscosity fluid when the Rayleigh number is defined in terms of the viscosity corresponding to a temperature equal to the average of the boundary temperatures. The relationship between Nusselt number and supercriticality (R_a/R_c) is even more remarkable being independent of viscosity variation and indistinguishable from that of a uniform-viscosity fluid with appropriate Prandtl number. The horizontally averaged temperature becomes increasingly asymmetrical with increasing viscosity variation due to the relatively large temperature change across the cold, more-viscous boundary layer, and results in an isothermal interior temperature significantly hotter than the average of the boundary temperatures. The measured temperature and convective heat transfer as a function of depth show that for viscosity variations greater than about 100 most of the viscosity change occurs within a stagnant conductive layer that develops above the actively convecting part of the system.

1. Introduction

The understanding of convection in large-Prandtl-number Boussinesq fluids with uniform properties and contained in simple geometries is virtually complete. Analytic methods (Malkus & Veronis 1958; Kuo 1961; Busse 1967*a*), laboratory experiments (Rossby 1969; Krishnamurti 1970; Busse & Whitehead 1971) and numerical solutions (e.g. McKenzie, Roberts & Weiss 1974) provide a thorough description of the flow and thermal structure, the heat-transfer efficiency and the planform of such convection. Present efforts are typically directed towards relaxing some of the original assumptions by going to lower Prandtl number, more complicated geometries,

† Permanent address: The University of Chicago, Chicago, Illinois.

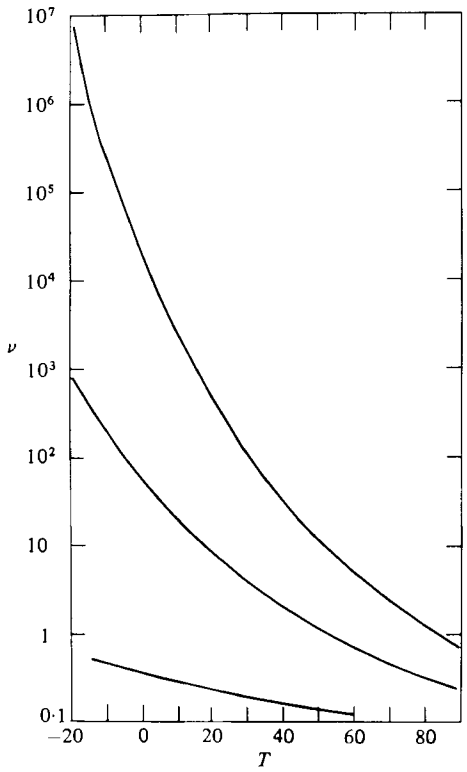

FIGURE 1. Kinematic viscosity in stokes as a function of temperature in °C for silicone oil (smallest viscosity), L-100 (intermediate viscosity), and golden syrup (which has the largest viscosity).

variable material properties, or introducing new dynamical processes such as the Lorentz forces.

The experiments described in this paper address the effect on convection of relaxing the assumption of a uniform viscosity. The material properties of all real fluids depend to some extent on their thermodynamic state, and in the case of viscosity it can vary by many orders of magnitude; the most notable example of this being convection in a planetary interior where the deformation is due to thermally activated solid-state creep. In the case of the Earth, plate tectonics and its corollary of a deformable mantle are clear evidence of the importance of convection for the structure and evolution of its thermal state, but a central feature of such convection, that the viscosity (or effective viscosity in the case of a nonlinear rheology) varies by about an order of magnitude for each change of 100 °C, has received very little attention. At present the enormous viscosity variations associated with convection in a planetary interior are dealt with by assuming a two-layer representation of an effectively isoviscous flow under a high-viscosity conductive lid (e.g. Richter & McKenzie 1981). This approach, while producing some rationalization of the geological estimates of temperatures at depth in the Earth, does depend on an assertion about the behaviour of variable-viscosity fluids which as yet has little if any theoretical or experimental basis. The reason for this situation is not lack of effort, but the inadequacy of most existing methods for covering a sufficiently large range of the relevant parameters. Analytic methods (Busse 1967*b*) are restricted to small viscosity variations and small amplitude. Numerical methods (Torrance & Turcotte 1971; Daly

1978) serve mainly to bring out qualitative features (the development of a cold, stagnant, high-viscosity region near the surface and a thinning of the upwelling regions compared to the downwellings) since they develop severe resolution problems once either the Rayleigh number or the viscosity variation becomes large. This leaves for the moment laboratory experiments as the most promising tool, especially since readily available fluids such as Tate & Lyle's golden syrup and polybutene oil have viscosities that vary by many orders of magnitude for the temperature changes achieved in the laboratory (figure 1).

The experiments reported here were designed to measure both the horizontally averaged temperature as a function of depth and the heat transfer of convection over a range of viscosity variations up to 10^5. The heat-transfer results, parametrized in terms of a Nusselt-number–Rayleigh-number relation, relate the temperature drop across the layer to the mean heat flux and therefore are useful for estimating temperatures at depth from heat-flow measurements made at the surface of a natural system whose viscosity depends on temperature. For uniform-viscosity fluids the surface temperature together with the Nusselt number are sufficient to determine a reasonably accurate and complete temperature profile by extending the temperature gradients at the boundaries until they intersect the interior temperature, which is close to isothermal and equal to the mean of the boundary temperatures. The situation is more complicated in a variable-viscosity fluid because the interior temperature structure while still approximately isothermal is no longer equal to the mean of the boundaries. This is demonstrated by the measured horizontally averaged temperature profiles, which are also needed to determine the viscosity structure associated with the convective state.

As to the planforms of the convective state in our experiments, we refer the reader to the work of White (1982), which is an important complementary study to our own. In general the cells are three-dimenstional: hexagons, squares or imperfect polygons, with typical dimensions equal to or slightly smaller than the layer depth.

2. Linear theory

The linear stability of various variable-viscosity fluids is discussed in detail by Stengel, Oliver & Booker (1982), and thus we limit ourselves here to those aspects that are useful for understanding or normalizing the experimental results. The linear theory is relevant in several important ways. It is needed in connection with the experiments for the onset of convection with large viscosity variation, which demonstrate that the process is one of finite-amplitude instability occurring at Rayleigh numbers below the critical value. Despite this the critical Rayleigh number provides a simple way of incorporating the effect of variations in viscosity when parametrizing the heat transfer in terms of the Rayleigh number. Finally the eigenfunctions of the linear problem suggest that once the viscosity variations are sufficiently large the system can be usefully represented as a convective layer below a conductive lid.

The critical Rayleigh number of three different viscosity laws for a non-rotating Boussinesq layer of fluid between rigid isothermal boundaries is given in figure 2. The definition of Rayleigh number used is

$$R_a = \frac{g\alpha\,\Delta T d^3}{\kappa \nu_{\frac{1}{2}}}, \tag{1}$$

where g is the acceleration due to gravity, α is the coefficient of thermal expansion,

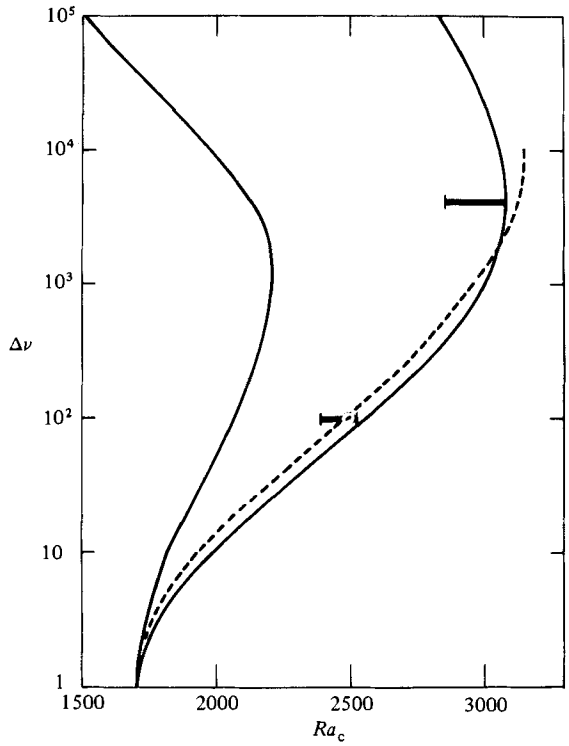

FIGURE 2. Critical Rayleigh number as a function of the total viscosity variation for an exponential fluid (solid curve on the left), L-100 with mean temperature of 25 °C (dashed) and golden syrup with bottom temperature of 82 °C. $\Delta\nu$ is the ratio of the maximum to minimum viscosity in the system. The heavy horizontal line at $\Delta\nu = 100$ gives the range of critical Rayleigh numbers for L-100 with mean temperature between 15 °C and 40 °C. The heavy line at $\Delta\nu = 4 \times 10^3$ gives the range of critical Rayleigh numbers for golden syrup with bottom temperature between 60 °C and 82 °C.

ΔT is the vertical temperature change, d is the depth, κ is the thermal diffusivity and $\nu_{\frac{1}{2}}$ is the kinematic viscosity corresponding to a temperature equal to the mean of the two boundary temperatures. The exponential fluid has a viscosity structure

$$\nu_{(z)} = \nu_{\frac{1}{2}} e^{c(z-\frac{1}{2})}, \quad c = \ln \Delta\nu, \tag{2}$$

where z has been non-dimensionalized using the depth, and $\Delta\nu$ is ratio of maximum to minimum viscosity in the system, which occur at the boundaries. L-100 and golden syrup have dimensional viscosity laws (see figure 1) that are accurately represented by a relation of the form

$$\psi_{(T)} = a \exp\{b\, e^{-T/c}\}, \tag{3}$$

with $a = 0{\cdot}02985$, $b = 7{\cdot}55$, $c = 68{\cdot}8$ °C for L-100 and $a = 0{\cdot}1138$, $b = 12{\cdot}3$, $c = 51{\cdot}3$ °C for golden syrup. The curve for L-100 in figure 2 assumes that $\nu_{\frac{1}{2}}$ is the viscosity at 25 °C, while the golden syrup curve is for a fixed bottom temperature of 82 °C. A fixed mean or boundary temperature is needed in the case of superexponential viscosities for a smooth curve of critical Rayleigh number *vs.* viscosity ratio $\Delta\nu$.

The critical-Rayleigh-number curve for the exponential fluid is the same as found by Stengel *et al.* (1982) and shows how the critical Rayleigh number is increased above that of a layer with uniform viscosity $\nu_{\frac{1}{2}}$ for $\Delta\nu < 10^4$. At larger viscosity variations

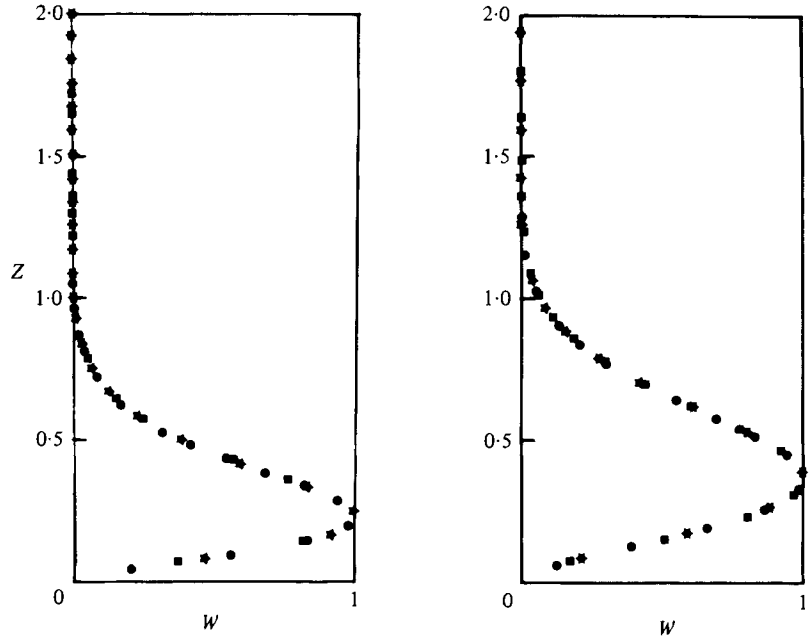

FIGURE 3. Vertical velocity eigenfunctions (normalized to a maximum value of unity) for an exponential viscosity law (on the left) and golden syrup (on the right) as a function of a stretched vertical coordinate as described in the text. Three different viscosity ratios are plotted in each case: $\Delta\nu = 10^4$ (●), 10^6 (■) and 10^8 (★).

the critical Rayleigh number becomes smaller because convection begins in a low-viscosity sublayer. The situation with the superexponential fluids is similar but the increase in critical Rayleigh numbers is more pronounced. The experiments for the onset of convection in golden syrup show that convection exists at Rayleigh numbers significantly lower than the critical value given in figure 2.

The confinement of convection to a low-viscosity sublayer can be illustrated using the vertical velocity eigenfunctions of cases with large viscosity variation. In the case of the exponential fluid a sublayer Rayleigh number can be defined:

$$R_a = \frac{g\alpha\Delta T z^4}{\kappa\nu_{z/2}}, \tag{4}$$

where $\nu_{z/2}$ is the viscosity at the midpoint of the sublayer of depth z. For large viscosity variations ($> 3\times10^3$) this Rayleigh number is always maximized by the sublayer that has a viscosity variation of exactly e^8, corresponding to a sublayer thickness of $8/\ln\Delta\nu$. If convection is confined to this sublayer, the vertical velocity eigenfunctions as a function of a new stretched coordinate $\hat{z} = \frac{1}{8}z\ln\Delta\nu$ should be the same for all $\Delta\nu$ and vanish at $\hat{z}\approx 1$. That this is the case for large viscosity variations is shown in figure 3. Similar arguments for L-100 and golden syrup result in a stretched coordinate

$$\hat{z} = z\ln\left[1+\frac{\ln\Delta\nu}{b\,e^{-T/c}}\right], \tag{5}$$

where b and c are the constants associated with the viscosity law and T is the temperature at the bottom of the layer. The vertical velocity eigenfunctions for golden syrup with a bottom temperature of 82 °C in terms of $\hat{z}$ are shown in figure

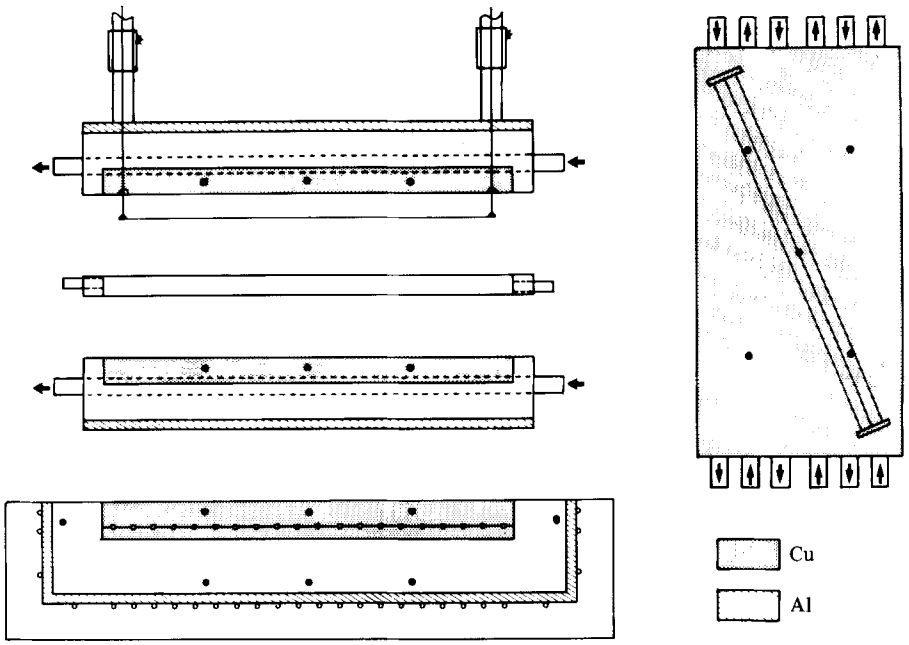

FIGURE 4. Schematic diagrams of the various elements that can be combined to make a convection apparatus. (*a*) Side view of the isothermal top including the platinum wires stretched between nylon spacers attached to the shaft of calipers. The position of thermocouples within the copper block is indicated by the small black circles. The copper block and pipes carrying thermostated water are surrounded by Plexiglas backed by an aluminium plate machined to be parallel to the exposed copper surface. (*b*) Plexiglas frame used to contain the fluid. The walls are 1 cm thick and have two openings used for filling the tank once it is assembled. (*c*) Isothermal copper block similar to (*a*) but without the platinum wires, which can be used as an isothermal base or top. (*d*) Electrically heated copper base with guard heaters. The nichrome heating wires are indicated by open circles. The heated copper block is surrounded by Plexiglas backed by aluminium plates whose temperature is controlled by separate heating wires. These guard heaters are covered by additional Plexiglas. The temperature of the copper block and surrounding Plexiglas is measured by thermocouples at the places indicated by the black circles. (*e*) Plan view of the top copper block showing the platinum wires, the position of the thermocouples, and the six copper tubes through which thermostated water flows in the direction indicated by the arrows. All diagrams are drawn to the same scale. The dimensions of the isothermal copper blocks are 20 cm × 10 cm × 1·25 cm.

3. The general result, at least for the marginal state, is that convection is confined to a sublayer with a fixed viscosity variation across it of e^8 (2981) for an exponential fluid and about 500 for golden syrup. The finite-amplitude state seen in the experiments can be similarly characterized, but the variation of viscosity across the convecting region is considerably smaller.

3. Experimental apparatus and fluids

The experiments, designed to measure the horizontally averaged temperature and convective heat transfer with an accuracy of about one percent, involve four fluids: water and silicone oil for comparison with the earlier results of Rossby (1969); L-100 polybutene oil and golden syrup for their strongly temperature-dependent viscosity.

Depending on the object of a particular set of experiments, various of the elements shown in figure 4 are combined. What we call the horizontally averaged temperature

is measured by the electrical resistance of three platinum wires stretched between nylon spacers attached to the shaft of calipers that accurately control the position of the wires. The calipers are mounted on a $20 \times 10 \times 1{\cdot}25$ cm copper block used as the upper isothermal boundary for the fluid layer. The temperature of this block, and that of a similar copper block used as a bottom boundary, is measured in five places by thermocouples and controlled by thermostated water flowing through copper tubing welded into channels cut in the back of each block. The water flow is in opposite directions in adjacent tubes to minimize horizontal temperature gradients due to heat transfer into or out of the fluid layer. The fluid is contained by a Plexiglas frame cemented with a silicone adhesive to the copper boundaries. Each of the copper blocks is surrounded (except for their front surface) with Plexiglas backed by an aluminium plate machined to be perfectly parallel to the front surface of copper. These aluminium plates allow the assembled tank to be levelled and are also used to measure the depth of the fluid layer, which is always slightly greater than the height of the containing frame because of the silicone cement.

The thermocouples measuring the temperature of the copper boundaries have their reference junction in a bath whose temperature is known to better than $\pm 0{\cdot}01$ °C. The thermojunction voltage is measured with a Keithley 191 digital multimeter with 1 μV resolution. Each thermocouple is stable to ± 1 μV ($\approx 0{\cdot}025$ °C) and the greatest difference between any two thermocouples within a single block was 2 μV. This difference is always the same and therefore is probably due to differences between the thermocouples themselves and not horizontal temperature gradients. The initial calibration and the uniformity among the five thermocouples suggests that the temperature of the boundaries is maintained and known to better than 0·1 °C.

A potential source of error is the depth the fluid layer. The Plexiglas frames are carefully machined but the silicone cement used to assemble the apparatus increases the depth by a small but significant amount. The separation of the aluminium plates provides one measure of the fluid-layer depth and shows that the cement adds $0{\cdot}04 \pm 0{\cdot}02$ cm to that of the frame, which is 1·00 or 2·35 cm depending on which fluid is used. A second way of measuring the depth is to extrapolate a conductive temperature gradient measured with the platinum wires until it intersects the known boundary temperature. Both methods of measuring the depth indicate that the depth is uniform and known to within 0·02 cm.

The resistance of the platinum wires is measured with the same Keithley instrument, which has a resolution of 1 mΩ ($\approx 0{\cdot}02$ °C). The calibration of resistance in terms of temperature is first carried out under isothermal conditions to determine the effect of moving the wires up and down in the fluid layer. The resistance measured at intervals of 0·02 cm varies slightly with depth, which we attribute to changes in tension. The changes in measured resistance are greatest near the upper boundary where the difference is equivalent to 1 °C over the first 0·1 cm but only 0·1 °C per centimetre below this depth. The rapid change in resistance near the upper boundary seems to be associated with stretching of the wires when the nylon spacers are drawn into spaces cut into the boundary that allow them to be raised far enough so that the platinum wires can be brought very close to the upper boundary. The isothermal calibrations were carried out over a range of temperatures and the effect of changing depth remained the same; therefore a simple correction can be made.

A second set of calibrations using stable conductive gradients was carried out to determine the accuracy of the position of the wires, and also as mentioned above, to provide an estimate of the total layer depth. The two sets of calibrations result in an estimated accuracy of $\pm 0{\cdot}1$ °C for the horizontally averaged temperature. The

vertical temperature gradient derived from temperature measurements at closely spaced depth intervals is accurate to better than 5% except very close to the boundaries where the effect of changing tension reduces the accuracy.

The problems of accurately measuring the temperature gradient at the boundaries makes it necessary to use a different system for determining the rate of heat transfer across the layer. A copper block containing a direct-current nichrome heating element replaces the isothermal base. The power input to the heater is determined by separately measuring the voltage across the heater and across a precision resistor placed in series that gives the current. The heated copper block is surrounded by 1 inch Plexiglas backed by aluminium plates containing independently controlled guard heaters that reduce the temperature gradient and associated heat loss across the Plexiglas to a negligible amount. The advantage of guard heaters over heavy thermal insulation is in the much-shorter time constant for the system as a whole to reach thermal equilibrium. The thermostated copper block without the platinum wires is now used for the top boundary and as before the fluid is contained with a Plexiglas frame.

The main source of error in the heat transfer measurements is due to conduction by the Plexiglas frame. To correct for this the apparatus is first calibrated by turning it upside down and running stable conductive experiments. The heat transfer by the sidewalls H_{sw} is then the difference between the power input to the heater H and that transmitted conductively across the fluid layer of area A, depth d, thermal conductivity K and temperature difference ΔT. If necessary, correction for heat loss from the main heater to the sides H_s and to the bottom H_b can be made, and these are never greater than 1% and typically 0·1% of H. The heat carried by the frame containing the fluid is

$$H_{sw} = H - \frac{AK\Delta T}{d} \pm H_s \pm H_b. \tag{6}$$

Repeated experiments with different power inputs showed that $H_{sw}/\Delta T$ is quite constant for a given assembled tank and fluid, and can be used as a correction for the convective-heat-transfer experiments. For a typical case the heat carried by the sidewalls is of order 1% of the total heat input in the case of water and 5% for the other fluids. An important imponderable is that the correction is obtained from a conductive situation and applied to convective cases having larger heat flux and no longer the same temperature structure as the sidewalls. Furthermore the correction requires an independent estimate of K, a quantity that is in some cases poorly known. Partly because of the uncertainties introduced by the sidewalls, we decided to include the experiments using water and silicone oil, which when compared to the results of Rossby (1969) serve to some extent as an additional calibration of the experimental design and procedure. The accuracy with which we believe we are measuring the heat transfer varies from fluid to fluid and therefore we will discuss it later together with the actual results.

The properties of the four fluids used in the experiments are given in table 1. Of these fluids water is the most common and accordingly its properties are the least uncertain. The values listed for water are the standard ones used by the Hydrodynamics Laboratory at the University of Chicago (Dave Fultz, private communication) and are not significantly different from those used by Rossby (1969). In the case of silicone oil (20 cSt Dow Corning 200 Fluid) we measured its viscosity, using a Haake falling-ball viscometer accurate to better than 1%, its density and thermal expansion; the other listed properties being those given by the manufacturer.

The material properties for L-100 (a polybutene oil manufactured by AMOCO)

Property at 20 °C	Water	Silicone oil	L-100	Golden syrup	Units
Density (ρ)	0·9983	0·9534	0·8655	1·438	g cm^{-3}
$d\rho/dT$	$-2{\cdot}00\times10^{-3}$	$-1{\cdot}02\times10^{-3}$	$-5{\cdot}9\times10^{-4}$	$6{\cdot}22\times10^{-4}$	g cm^{-3} °C^{-1}
Thermal conductivity (K)	$5{\cdot}87\times10^{-3}$	$1{\cdot}41\times10^{-3}$	$1{\cdot}085\times10^{-3}$	$3{\cdot}17\times10^{-3}$ ($3{\cdot}53\times10^{-3}$)	W cm^{-1} °C^{-1}
dK/dT	$1{\cdot}65\times10^{-5}$	0	$1{\cdot}0\times10^{-6}$	$1{\cdot}0\times10^{-5}$ ($1{\cdot}84\times10^{-5}$)	W cm^{-1} °C^{-2}
Specific heat C_p	4·1819	1·447	1·942	2·02	J g^{-1} °C^{-1}
dC_p/dT	$6{\cdot}0\times10^{-4}$	0	$4{\cdot}05\times10^{-3}$	0	J g^{-1} °C^{-2}
Kinematic viscosity ν	$1{\cdot}01\times10^{-2}$	$2{\cdot}34\times10^{-1}$	8·40	$4{\cdot}75\times10^{2}$	cm^2 s^{-1}
Prandtl number ν/κ	7·16	$2{\cdot}29\times10^{2}$	$1{\cdot}30\times10^{4}$	$4{\cdot}35\times10^{5}$ ($3{\cdot}91\times10^{5}$)	—

TABLE 1. Material properties

listed in table 1 are a mixture of our own measurements, values given by the manufacturer, and an independent measurement of the thermal conductivity made by Dynatech Research and Development Co. on a sample we provided. We measured the density and thermal expansion because Booker (1976) and Liang & Acrivos (1970) disagreed on the exact value of the thermal expansion of a similar polybutene oil (no. 8, Oronite Division of Standard Oil of California). Our value for the thermal expansion of L-100 is within 2 % of Booker's for no. 8. In the case of thermal conductivity we began by using the value given by the manufacturer, which is the same as the value adopted by Booker (1976) and Liang & Acrivos (1970). With this value of K we found a negative sidewall heat-transfer correction ($H_{sw}/\Delta T < 0$), which is impossible if the equipment is working correctly. The apparatus was taken apart, checked, reassembled, and filled first with water for a new measurement of $H_{sw}/\Delta T$. Without taking the apparatus apart, it was drained of water, dried, and refilled with L-100. Assuming that the $H_{sw}/\Delta T$ found with water applied also to L-100, a value for K was determined and found to be 23 % lower than the value given by the manufacturer. For fear of assuming too much, a sample of L-100 was sent to Dynatech for an independent set of measurements. The value of K given in table 1 is from the Dynatech report (quoted accuracy of ± 2 %). It is 3 % larger than our own estimate using the calibration with water, but 20 % lower than the manufacturer's value. The viscosity of L-100 (figure 1) was measured over the range of temperatures relevant to the experiments. The remaining properties listed in table 1 are those given by the manufacturer.

The situation for golden syrup is somewhat similar to that of L-100. The main source of concern is the thermal conductivity and its temperature dependence. Two values are given in table 1; the first is our own estimate using the water calibration procedure described above; the value in parentheses is from Wray (1974), which was measured at the National Physical Laboratory with a reported accuracy of ± 2 %. While we prefer our own estimate, the results for golden syrup will be given using both values to illustrate the effect of uncertainties in K on the heat-transfer results. The viscosity of golden syrup (figure 1) was measured at various temperatures and agrees with measurements made by White (1982). Because of the very high temperatures of some of the cases, the viscosity was remeasured at the end of the

experiments, and despite a distinctly darker colour of the syrup the remeasured viscosity was never more than 2·4 % from the original measured value. The density was also measured and agrees with the values reported by Wray (1974). The thermal expansion and specific heat are taken from Wray (1974).

The design of the experiments was based on a desire to achieve an accuracy of about 1 % when measuring either the horizontally averaged temperature as a function of depth or the rate of heat transfer. We believe this standard was achieved for the temperature measurements and for the relative changes in heat transfer associated with Rayleigh numbers and viscosity variation for each individual fluid. The absolute rate of heat transfer is less accurate in all cases except water because of the uncertainties of the material properties, especially the thermal conductivity.

4. Heat transfer

The non-dimensional heat flux or Nusselt number Nu can be defined in terms of the ratio of the temperature change across the layer needed to transport conductively a given quantity of heat to the convective temperature drop required for the same amount of heat. Thus

$$Nu = \frac{\Delta T_{\text{cond}}}{\Delta T_{\text{conv}}}, \tag{7}$$

$$\Delta T_{\text{cond}} = \frac{H_{\text{f}} d}{KA}, \tag{8}$$

$$H_{\text{f}} = H - \frac{H_{\text{sw}}}{\Delta T} \Delta T_{\text{conv}} \pm H_{\text{s}} \pm H_{\text{b}}. \tag{9}$$

H_{f} is the heat flux through the fluid determined by correcting the total power input H for heat carried by the Plexiglas sidewalls $((H_{\text{sw}}/\Delta T)\Delta T_{\text{conv}})$ and heat lost or gained by conduction in the Plexiglas surrounding the main heater (H_{s} and H_{b}). ΔT_{conv}, H and the temperature difference between the main heater and the guard heaters are measured, the thermal conductivity K is evaluated at the mean of the boundary temperatures, and $H_{\text{sw}}/\Delta T$, the depth d and the area A are constant for a set of runs using the same fluid and apparatus. The Rayleigh number of each experiment is determined using the fluid properties evaluated at the mean temperature of the boundaries.

5. Results for water and silicone oil

The experiments using water or silicone oil were run for comparison with the earlier results of Rossby (1969) and Krishnamurti (1970). Figure 5 shows our measured Nusselt numbers together with lines representing the relations

$$Nu = 0{\cdot}184 Ra^{0{\cdot}281} \quad \text{(silicone oil)}, \tag{10}$$

$$Nu = 0{\cdot}131 Ra^{0{\cdot}30} \quad \text{(water)}, \tag{11}$$

which are best fits to Rossby's data. In the case of water all our measurements are within 1 % of relation (11), while for silicone oil we are systematically lower by about 3 % compared with relation (10). The excellent agreement in the case of water is not surprising because the correction for heat transport by the sidewalls is small and the material properties are well known. The sidewall correction is much more important

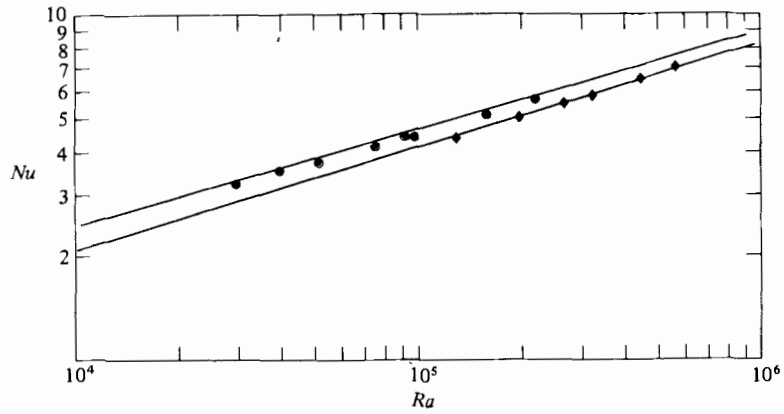

FIGURE 5. Nusselt numbers from experiments using water (◈) and 20 cSt silicone oil (◉) as a function of the Rayleigh number. The straight lines are best fits to the data of Rossby (1969) for the same two fluids.

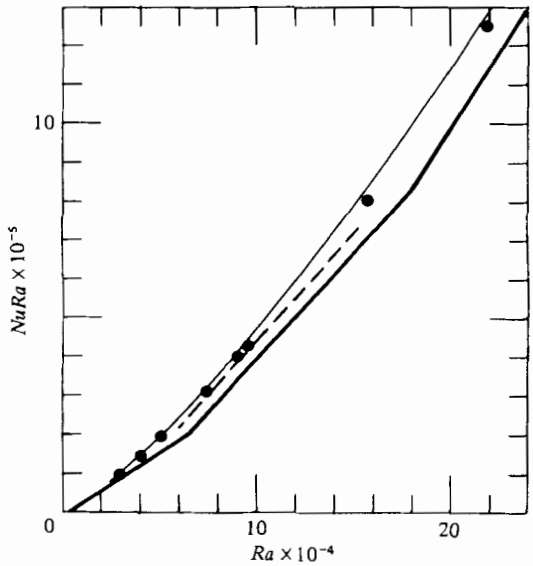

FIGURE 6. Rayleigh number times Nusselt number plotted against the Rayleigh number for experiments using silicone oil. ——, best-fitting curve to Rossby's (1969) data for 20 cSt silicone oil, which has a Prandtl number of about 200. ●, our own data for the same oil. ——, from Krishnamurti (1970) for 10 cSt (Prandtl number ≈ 100). – – –, from Krishnamurti (1970) for 1000 cSt silicone oil (Prandtl number ≈ 860).

when using silicone oil (as it is for L-100 and golden syrup) and the agreement between the two experiments is not as good. Krishnamurti's results together with Rossby's and our own are shown in figure 6 on a plot of Nusselt number times Rayleigh number *vs.* Rayleigh number, which is the form used by Krishnamurti. Assuming that 10 and 20 cSt silicone oils are comparable, Krishnamurti's results are about 10 % lower than those of the other two experiments. The main reason for the differences between the three experiments is almost certainly imperfect correction for heat transport in the sidewalls and thermal insulation.

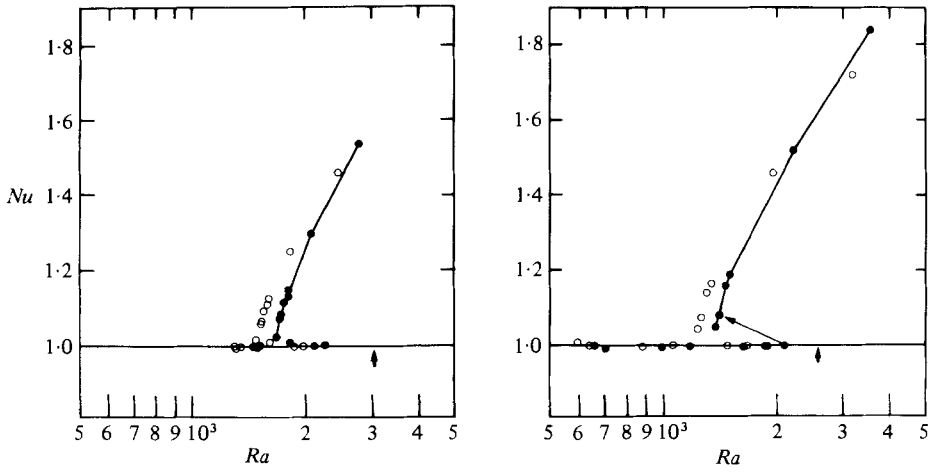

FIGURE 7. Nusselt numbers from experiments using golden syrup and with Rayleigh number near critical. (*a*) Cases with viscosity variations between $2{\cdot}6 \times 10^3$ and $3{\cdot}8 \times 10^3$. The solid (open) symbol means that the smaller (larger) value of thermal conductivity from table 1 was used. The vertical arrow indicates the critical Rayleigh number given by the linear theory. (*b*) Same as (*a*) but for viscosity variations between 9×10^4 and $5{\cdot}7 \times 10^5$. The long arrow pointing towards the left joins a conductive point that persisted for about 12 hours before going unstable to the convective point, which has the same total heat flux.

Comparing the three experiments emphasizes the distinction between precision and accuracy. Our experiments have a precision of about 1 % judged by the scatter around the relation

$$Nu = 0{\cdot}18 Ra^{0{\cdot}281}. \tag{12}$$

The absolute accuracy, which is mainly a matter of resolving the multiplying constant, is much more uncertain, and given the differences between the experiments might be no better than 10 %. We will use (12) as the uniform-viscosity relationship with which to compare the variable-viscosity results. There is an added complication in that (12) is for a Prandtl number of about 200, while L-100 and golden syrup have Prandtl numbers two to three orders of magnitude greater. From figures 5 and 6 one can see that the Nusselt number at fixed Rayleigh number increases with increasing Prandtl number, thus the Nusselt numbers given by (12) will be lower than the approprate value for a uniform-viscosity fluid with a Prandtl number equal to that of L-100 or golden syrup.

The overall conclusion is that the precision of the experiments is quite sufficient to resolve changes in the Nusselt number due to different Rayleigh numbers (or, later, viscosity variations), but that the accuracy is not well enough known to attach much significance to differences of less than 10 % in the actual value of the Nusselt number between experiments using different fluids or even different experiments using the same fluid.

6. Results near critical

Two sets of experiments with fixed viscosity variation of about 3×10^3 and 10^5 were run using golden syrup to determine the Nusselt number for Rayleigh numbers near critical. Busse's (1976*b*) theoretical analysis for small-amplitude convection with weak viscosity variations suggests that convection can exist at subcritical Rayleigh

numbers, and we wanted to demonstrate this point in the case of large viscosity variations when the effect would be most easily observed. The experimental results are given in figure 7, and in each case two values of the thermal conductivity are used to show that the uncertainty in K is not very important.

Each set of experiments began with convection well established ($Nu > 1{\cdot}5$). The heat input was then reduced in steps with sufficient time between changes to insure that a new steady state was established. Since the adjustment time of convection at small Rayleigh numbers can be very long, two or more measurements of the Nusselt number, separated by at least four hours, were made to confirm that the system was indeed steady. The data for both cases fall along curves that intersect a Nusselt number of unity at Rayleigh numbers of about half the critical value. After several Nusselt-number measurements at Rayleigh numbers less than this intersection value, the heat input was increased in steps and the conductive state ($Nu = 1$) was found to persist at Rayleigh numbers that earlier had been clearly convective. This conductive state finally breaks down with further increases in the heat input at Rayleigh numbers still below the critical value found in the linear theory. The onset of convection makes the Nusselt number jump back onto the original curve and is accompanied by a reduction in the Rayleigh number due to the smaller temperature change across the convecting layer and an associated increase in the viscosity used in the definition of the Rayleigh number. Had we controlled the boundary temperatures instead of the heat input, the data points would have been the same, but the jump in Nusselt number would have been at constant Rayleigh number.

The finite-amplitude instability implicit in the behaviour of the Nusselt number near critical is almost certainly due to the effect of variable viscosity. No such behaviour is seen in more nearly uniform viscosity fluids such as water and silicone oil (Rossby 1969); in fact the extrapolation of the Nusselt-number–Rayleigh-number curve to a Nusselt number of one gives a very good estimate of the critical Rayleigh number in these fluids. That it is not the case for fluids with strong temperature-dependent viscosity is not surprising (Busse 1967). The breakdown of the conductive state well below the critical Rayleigh number is probably influenced by the sidewalls containing the fluid. White (1982) has observed the onset of convection at subcritical Rayleigh numbers when the viscosity variation is 50 and finds that cells develop first along the sidewalls and then slowly diffuse into the interior. Such an evolution is consistent with the sidewalls providing finite-amplitude disturbances that grow at Rayleigh numbers below critical.

7. Results for L-100 and golden syrup

Nusselt numbers from experiments with L-100 and golden syrup can be used to determine a representative viscosity, which when used to calculate the Rayleigh number results in a Nusselt-number–Rayleigh-number relationship such as (12). By representative we mean that the parametrized heat transfer is as much as possible independent of the viscosity variation.

An obvious choice for a representative viscosity is that corresponding to a temperature equal to the mean of the boundaries ($\nu_{\frac{1}{2}}$), which was used earlier for defining the Rayleigh number in the linear theory. Booker (1976) has already shown that this viscosity leads to a Nusselt-number–Rayleigh-number relation that predicts the measured heat transfer of a variable-viscosity fluid with $\Delta\nu$ up to 350 to within 15%. We can now test this result over a much larger range of $\Delta\nu$. A useful way of displaying the results is to normalize the measured Nusselt number by dividing it

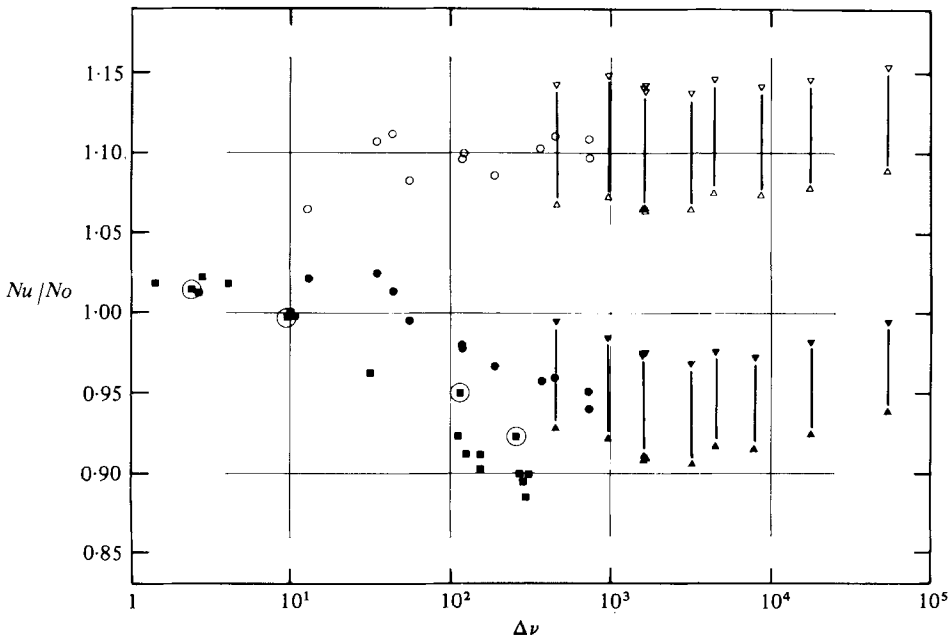

FIGURE 8. Normalized Nusselt numbers as a function of the total variation in viscosity. The solid symbols are for the Nusselt number divided by the value given by (12), while the open symbols use (13) to normalize the measured Nusselt number. ■, data from Booker (1976); ●, ○, L-100; ▼, ▽, golden syrup. Two values are plotted for each experiment using golden syrup: the larger (smaller) value used the smaller (larger) value of thermal conductivity given in table 1. The four squares with circles around them are those experiments by Booker for which the Rayleigh number is less than $2{\cdot}3 \times 10^4$.

by the Nusselt number from (12) when $\nu_{\frac{1}{2}}$ is used to calculate the Rayleigh number. The solid symbols in figure 8 show the normalized Nusselt numbers for L-100, golden syrup and Booker's (1976) data, over a range of almost five orders of magnitude in viscosity variation. The general conclusion is as before: $\nu_{\frac{1}{2}}$ is indeed a representative viscosity in that the variable-viscosity fluids have a non-dimensional heat transfer within 20% of that of a uniform viscosity equal to $\nu_{\frac{1}{2}}$.

In detail there are various points worth mentioning about the data in figure 8. The L-100 data when extrapolated to a uniform viscosity ($\Delta\nu = 1$) have a normalized Nusselt number of about 1·1, which is not unreasonable since the uniform-viscosity reference given by (12) is for a much lower Prandtl number. Krishnamurti's (1970) data for the Nusselt number of silicone oils with Prandtl numbers 100 and 860 suggest that a difference of about 10% is more or less what one should expect. Booker's (1976) data obtained with a polybutene oil very similar to L-100 are lower in absolute terms than our own, but do show a similar dependence of the normalized Nusselt number on $\Delta\nu$. We believe that Booker's (1976) data are too low because his assumed value of the thermal conductivity is incorrect, as we mentioned earlier when discussing the material properties of the experimental fluids. Given the reference used, the fact that his data extrapolate to a normalized Nusselt number of unity is added reason to believe that they are too low. It is worth noting that Booker (1976) did not measure the heat transfer of silicone oil himself, and therefore his experiments are not directly calibrated in terms of the reference fluid. His data have one advantage over ours in that they cover a large range of Rayleigh numbers. For each experiment using golden

syrup we have plotted two values of the normalized Nusselt number, corresponding to the two values of the thermal conductivity given in table 1. Again there is an uncertainty in the actual level of the normalized Nusselt number, but its trend with viscosity variation is not significantly affected by the choice of K. If forced to choose, the higher value for golden syrup is more likely to be correct on the basis that it should have a slightly higher normalized Nusselt number than L-100 because of its greater Prandlt number.

Booker & Stengel (1978) have suggested an even more striking normalization for the Nusselt numbers of variable-viscosity fluids by using the degree of supercriticality in place of the Rayleigh number alone in relation (12). For a uniform-viscosity fluid (12) can also be written

$$Nu = 1{\cdot}46\left(\frac{R_a}{R_c}\right)^{0{\cdot}281}, \tag{13}$$

where R_c is the critical Rayleigh number. When this relation is applied to a variable-viscosity fluid the critical Rayleigh number contains the information on the degree of viscosity variation. The measured Nusselt numbers for L-100 and golden syrup normalized by (13) are shown by the open symbols in figure 8. Aside from uncertainties in the actual level, the normalized Nusselt numbers are now virtually independent of viscosity variation. A remarkable result when one considers that the actual viscosity varies in some cases by five orders of magnitude.

8. Horizontally averaged temperature

Examples of the non-dimensional horizontally averaged temperature at large Rayleigh number are shown in figure 9, and at lower Rayleigh number, but covering a greater range in viscosity variations, in figure 10. The most obvious feature resulting from the variations in viscosity is the asymmetry between the hot and cold boundary layers and associated offset of the interior temperature from the average of the two boundary temperatures. In terms of the earlier results on heat transfer that emphasized the importance of $\nu_{\frac{1}{2}}$, we now see that this viscosity is not that of the isothermal interior: instead it corresponds to a level somewhere in the upper cold boundary layer where the temperature is equal to 0·5. The offset of the interior temperature θ_i (θ_i is defined as the temperature at the inflexion point of the averaged temperature profile) from its uniform viscosity value of 0·5 is shown in figure 11 for a variety of Rayleigh numbers and viscosity variations up to 10^5. θ_i increases smoothly with increasing viscosity variation but discontinuously with Rayleigh number. At small Rayleigh numbers (10^4–2×10^4) the interior temperature falls along the solid curve. At Rayleigh numbers in the range 2×10^4–4×10^4 the interior temperature increases with increasing Rayleigh number with the data falling between the solid and dashed curves. At Rayleigh numbers greater than 4×10^4, and up to 8×10^5, the interior temperature becomes independent of R_a and falls along the dashed curve. This dependence on Rayleigh number suggests a transition at Rayleigh numbers in the range 2×10^4–4×10^4 and independent of viscosity variation. White (1982) describes a change in planform from square cells with rising in their centres to a spoke pattern characterized by irregular polygons at Rayleigh numbers near 3×10^4 and viscosity variation greater than 20. This change in planform seems the most likely explanation for the change in interior temperature. We cannot use our own Nusselt-number data to address the change in heat transport associated with this transition because all our experiments are at Rayleigh numbers corresponding to offsets along the solid curve in figure 11. Booker's (1976) data cover a larger range

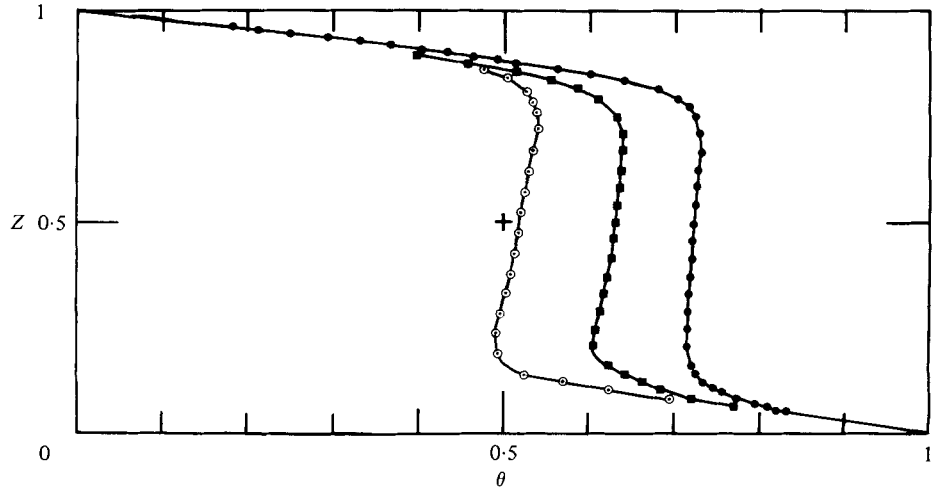

FIGURE 9. Non-dimensional tempterature θ as a function of depth. ○, 20 cSt silicone oil, $\Delta\nu = 3$, $R_a = 2{\cdot}16 \times 10^5$; ■, L-100, $\Delta\nu = 22$, $R_a = 1{\cdot}36 \times 10^5$; ●, L-100, $\Delta\nu = 750$, $R_a = 4{\cdot}95 \times 10^5$. In all but the last case data near the boundaries has been omitted.

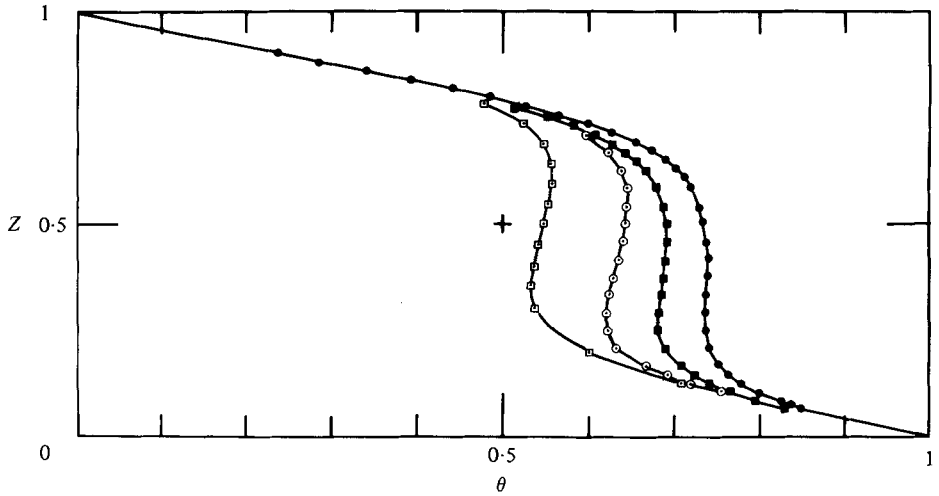

FIGURE 10. Non-dimensional temperature θ in L-100 and golden syrup as a function of depth for different total viscosity variation. □, L-100, $\Delta\nu = 11{\cdot}8$, $R_a = 2{\cdot}36 \times 10^4$; ○, L-100, $\Delta\nu = 10^2$, $R_a = 2{\cdot}29 \times 10^4$; ■, golden syrup, $\Delta\nu = 4{\cdot}15 \times 10^3$, $R_a = 1{\cdot}34 \times 10^4$; ●, golden syrup, $\Delta\nu = 10^5$, $R_a = 1{\cdot}02 \times 10^4$. Each symbol represents a measurement, and in all but the last case data near the boundaries has been omitted.

of Rayleigh numbers and two of his low-Rayleigh-number experiments ($R_a \approx 2 \times 10^4$, $\Delta\nu \approx 100$) have slightly larger (about 4 %) normalized Nusselt number than the higher-Rayleigh-number cases with similar $\Delta\nu$ (see figure 8). If this difference is real the effect of the transition is to reduce the heat-transfer efficiency as measured by the Nusselt number, as would be the case if the increase in the interior temperature is larger than the reduction in the temperature drop across the lower boundary layer resulting from the lower interior viscosity.

The horizontally averaged temperature profiles can be used to determine the

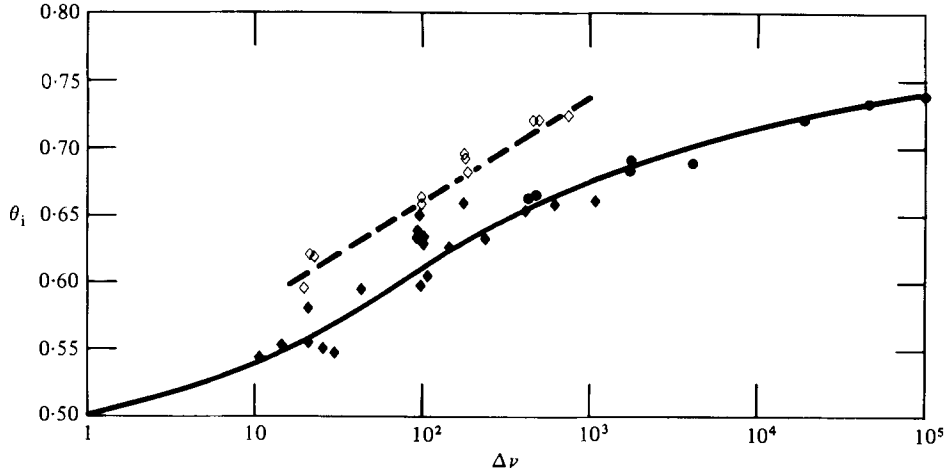

FIGURE 11. Non-dimensional interior temperature θ_i as a function of total viscosity variation. ◆, L-100, $R_a < 4 \times 10^4$; ◇, L-100, $Ra > 10^4$; ●, golden syrup, $R_a < 3 \times 10^3$.

average viscosity structure and the convective heat transfer as a function of depth. The fraction of the total heat flux carried by convection $C_{(z)}$ is simply

$$C_{(z)} = \frac{Nu - d\bar{\theta}/dz}{Nu}. \tag{14}$$

Because the Nusselt number and the horizontally averaged temperature gradients $d\bar{\theta}/dz$ are measured in separate experiments, we use (13) to estimate the appropriate Nusselt number for the experiments providing the averaged temperature gradient. Four examples of the temperature, viscosity and fractional convective heat transfer are given in figure 12. The convective heat transfer shows that the system develops a relatively thick conductive lid ($C \approx 0$) at the cold upper boundary, which accounts for most of the asymmetry between the boundary layers. The convective heat transfer in this 'lid' is in three of the cases shown slightly negative, which if real implies that the main convective flow drives counter-rotating cells in the lid. The accuracy of the data is not sufficient for confidence in this result, and furthermore no such secondary cells are seen in the eigenfunctions of the linear theory. The important point established by the data is that the system can be characterized as having convection below a conductive lid whose thickness is determined by the ability of the convective flow to penetrate into a region of high viscosity.

The viscosity structure shows that most of the viscosity change occurs within the conductive lid. The change in viscosity across the convective portion of the system is always small (< 100), being smallest (about 10) at the highest Rayleigh numbers studied ($R_a \approx 5 \times 10^5$). This suggests that the limit of strongly temperature-dependent viscosity and large Rayleigh number might be relatively simple, characterizable as effectively isoviscous convection under a conductive lid whose viscosity variation is of no relevance. However, for such a representation to be useful one must understand in a generalizable way the mechanisms that determine the relative thickness of these two layers.

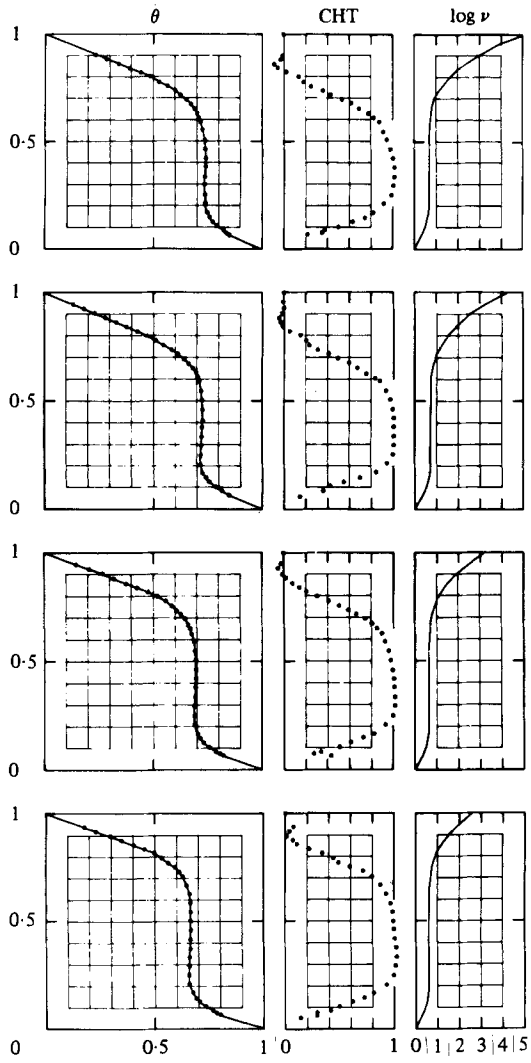

FIGURE 12. Non-domensional temperature θ, convective heat transport and viscosity normalized by its value at the bottom for experiments using golden syrup. Starting at the top the Rayleigh numbers are $1{\cdot}02 \times 10^4$, $1{\cdot}17 \times 10^4$, $2{\cdot}03 \times 10^4$ and $2{\cdot}67 \times 10^4$.

9. Discussion

The general approach adopted in this paper has been to compare the thermal properties of convection in variable-viscosity fluids to that of the uniform-viscosity case and seek a representative definition of the Rayleigh number such that parametrizing relationships like the dependence of Nusselt number on Rayleigh number retain their usefulness despite viscosity variations as large as five orders of magnitude. The viscosity $\nu_{\frac{1}{2}}$ corresponding to the mean temperature of the two boundaries leads to a representative Rayleigh number in that the corresponding critical Rayleigh number differs by no more than a factor of 2 from that of a uniform-viscosity fluid, and the heat transport as a function of this Rayleigh number is always within 20% of the corresponding constant-viscosity case. This heat-transfer result, first

demonstrated by Booker (1976) over a more limited range of viscosity variation, is now seen to hold for very large viscosity variations, which is remarkable indeed when one considers that $\nu_{\frac{1}{2}}$ is not necessarily associated with the region of active convection, and for viscosities variations only slightly larger than those studied will fall within the conductive lid that develops at the cold top boundary. $\nu_{\frac{1}{2}}$ will be within the conductive lid once the non-dimensional internal temperature exceeds 0·75. This leads one to suspect that the usefulness of $\nu_{\frac{1}{2}}$ might be specific to these particular fluids and the parameter range studied.

The dependence of the Nusselt number on the supercriticality of the layer (equation (13)), for which the effect of viscosity variation is contained in the critical Rayleigh number, is likely to be more general, but one should keep in mind that the viscosity structure of the conductive state on which the critical Rayleigh number is based is not the same as that of the convective state one is trying to describe. This distinction seems not to be important in the case of L-100 and golden syrup but it might become so for other temperature-dependent fluids. The success of using the supercriticality to determine the Nusselt number is somewhat surprising when one considers that there exists a finite-amplitude state when $Ra = R_c$ with Nusselt number as large as 1·6.

An alternative to seeking analogies between uniform- and variable-viscosity fluids is to emphasize their differences, in particular the existence of what we have called a conductive lid that accounts for the offset of the interior temperature from the average of the boundary temperatures. The usefulness of representing a variable-viscosity system in terms of a convective layer below a stagnant lid depends on understanding or at least being able to predict the relative thickness of the layers. In a sense the problem becomes one of penetrative convection, and the main result of the experiments is to show that the convective flow is restricted to a layer with a relatively small change in viscosity across it. The advantage of a two-layer representation is that it focuses on a specific issue, the ability of convection to penetrate into a high-viscosity region, which may prove easier to generalize than the concept of a representative Rayleigh number.

F.M.R. thanks the Royal Society for a guest research fellowship allowing him to spend a year at Cambridge University. This research was supported by the National Science Foundation grants EAR 79-26482 and EAR 82-00003.

REFERENCES

Booker, J. R. 1976 *J. Fluid Mech.* **76**, 741.
Booker, J. R. & Stengel, K. C. 1978 *J. Fluid Mech.* **86**, 289.
Busse, F. H. 1967*a* *J. Math. & Phys.* **46**, 140.
Busse, F. H. 1967*b* *J. Fluid Mech.* **30**, 625.
Busse, F. H. & Whitehead, J. A. 1971 *J. Fluid Mech.* **47**, 305.
Daly, S. F. 1978 Ph.D. dissertation, University of Chicago.
Krishnamurti, R. 1970 *J. Fluid Mech.* **42**, 309.
Kuo, H. L. 1961 *J. Fluid Mech.* **10**, 611.
Liang, S. F. & Acrivos, A. 1970 *Rheol. Acta* **9**, 447.
Malkus, W. V. R. & Veronis, G. 1958 *J. Fluid Mech.* **4**, 225.
McKenzie, D. P., Roberts, J. M. & Weiss, N. O. 1974 *J. Fluid Mech.* **62**, 465.
Richter, F. M. & McKenzie, D. P. 1981 *J. Geophys. Res.* **86**, 6133.

ROSSBY, H. T. 1969 *J. Fluid Mech.* **36**, 309.
STENGEL, K. D., OLIVER, D. S. & BOOKER, J. R. 1982 *J. Fluid Mech.* **120**, 411.
TORRANCE, K. E. & TURCOTTE, D. L. 1971 *J. Fluid Mech.* **47**, 113.
WHITE, D. 1982 Ph.D. dissertation, Cambridge University.
WRAY, F. 1974 Ph.D. dissertation, Cambridge University.